DOI: 10.61782/fa.2025.0134

FORUM ACUSTICUM
EURONOISE 2025

ANALYTIC EXPRESSIONS FOR THE LOW-FREQUENCY ACOUSTIC CENTER OF DIPOLE RADIATORS

Samuel D. Bellows[1*]

[1] Department of Electrical and Computer Engineering, University of Utah Asia Campus, South Korea

ABSTRACT

The concept of an acoustic center finds use in microphone calibration, evaluations of anechoic chambers, and modeling sound source directivity. Although precise definitions and interpretations vary between works, at low frequencies and for omnidirectional radiators, the acoustic center may be defined as the ratio of the dipole to the monopole moment of the source. This formulation provides a straightforward approach to represent the radiation from an extended source by a single monopole that preserves the amplitude and phase characteristics of the original source in the far field. However, not all sources are omnidirectional at low frequencies, including open-back guitar amplifiers, ported loudspeakers, cymbals, and gongs. This work extends the theory of the low-frequency acoustic center to such sources using the framework of multipole expansions. Spherical harmonic expansions of the pressure field measured using a spherical microphone array allow extraction of the multipole moments and the consequent acoustic center from measured data. Theoretical models, such as an axially vibrating cap on a sphere and an oscillating sphere, demonstrate the ability of the technique to model extended sources as a superposition of a monopole and dipole field.

Keywords: *acoustic center, sound source modeling, sound radiation, dipole radiation*

**Corresponding author*: samuel.bellows11@gmail.com.

1. INTRODUCTION

The concept of an acoustic center is relevant in applications varying from microphone calibration [1–3], anechoic chamber evaluation [4], and sound source modeling [5, 6]. However, the diverse definitions and conceptual postulations of the acoustic center's precise meaning across these applications has resulted in a similarly wide range of proposed algorithms. Jacobsen et al. [7] demonstrated that even for simple theoretical sources, the apparent location of the acoustic center depends on the specific definition employed, particularly at intermediate and high frequencies. This key finding underscores that the fundamental, yet often elusive, challenge is to determine how the acoustic center should be properly defined. Ideally, a robust definition of the acoustic center will lead to its consistent identification, regardless of the algorithmic approach used.

As thoroughly shown by Jacobsen et al. [7], the currently standardized definitions of the acoustic center [8, 9] fail to meet this criterion. Nonetheless, these standardized definitions do yield consistent results for sources which are omnidirectional radiators at low frequencies [10, 11]. At this *low-frequency acoustic center*, the extended, real source may be replaced by an single equivalent point source whose amplitude corresponds to the source's monopole moment. Reference [12] showed that approaches based on $1/r$ decays, phase shifts, or maximizing the energy in low order terms of a spherical harmonic expansion also converge to this same acoustic center location for both theoretical and real sources. Consequently, the concept of a low-frequency acoustic center qualifies as a robust definition because the same solution is obtained independent of the employed identification method.

Nonetheless, not all sources behave as monopoles at large wavelengths. These include sources with strong dipole moments such as ported loudspeakers and open-back guitar amplifiers [13, 14], cymbals and gongs [15], or even some stringed instruments with sound holes such as the violin [16]. Additionally, the concept of a low-frequency acoustic center cannot be applied to intermediate and high-frequency radiation with more complex radiation patterns. Determining a consistent definition of the acoustic center for all sources and for all frequencies requires further generalizations. This work explores the extension of the low-frequency acoustic center to dipole radiators. The approach adopts Vanderkooy's [10] principle of defining the low-frequency acoustic center through the multipole expansion of an extended source. However, rather than only considering a monopole radiator, the method retains both the monopole and dipole fields.

2. THEORY

2.1 Low-Frequency Dipole Acoustic Center

At low frequencies, or when the acoustic wavelength is much greater than the physical dimensions of the source, a multipole expansion of the Kirchhoff-Helmholtz Integral Equation leads to a simplified model of sound radiation [17]. This model forms by replacing the extended source with monopole, dipole, quadrupole, and higher-order radiators located at a single expansion point. The amplitude of these multipole components, or moments, depends on the choice of expansion point. A poor choice of expansion point can lead to a slowly converging series and large multipole moments [10]. In contrast, an optimal expansion point leads to a rapidly converging series with smaller multipole moments.

The low-frequency acoustic center for an omnidirectional source follows by choosing the expansion point to completely eliminate the dipole moment [10, 11]. However, not all sound sources behave omnidirectionally at low frequencies. Consider a source whose far-field pressure may be approximated by both a monopole and dipole field located at the acoustic center $\mathbf{r}_c$:

$$p(\mathbf{r}) = MG(\mathbf{r}, \mathbf{r}_c) + \sum_{\mu=1}^{3} D_\mu(\mathbf{r}_c) F_\mu(\mathbf{r}, \mathbf{r}_c). \quad (1)$$

In this equation,

$$M = iz_0 k \iint_S u_n(\mathbf{r}_s) dS \quad (2)$$

is the monopole moment, with k being the wavenumber, $z_0 = \rho_0 c$ the characteristic specific acoustic impedance, and u_n the normal particle velocity on the source's surface S. The function

$$G(\mathbf{r}, \mathbf{r}_0) = \frac{e^{-ikR}}{4\pi R}, \quad (3)$$

with $R = |\mathbf{R}|$, $\mathbf{R} = \mathbf{r} - \mathbf{r}_0$, is the free space Green's function, and

$$D_\mu(\mathbf{r}_0) = \iint_S iz_0 k u_n(\mathbf{r}_s)(x_{s\mu} - x_{0\mu}) + p(\mathbf{r}_s)\hat{n}_\mu dS \quad (4)$$

is the dipole moment in each of the three Cartesian coordinates $(x_1, x_2, x_3) = (x, y, z)$ with $\hat{n}_\mu$ representing the associated component of the surface unit normal vector [17]. Unlike the monopole moment, the dipole moment depends upon the choice of expansion origin $\mathbf{r}_0$. Lastly,

$$F_\mu(\mathbf{r}, \mathbf{r}_0) = ikG(\mathbf{r}, \mathbf{r}_0)\left(1 - \frac{i}{kR}\right)\hat{R}_\mu \quad (5)$$

is the dipole field in each direction [17].

If the coordinate system origin $\mathbf{r}_o = \mathbf{0}$ does not align with the acoustic center, then the multipole expansion will include higher order terms to ensure proper convergence. The quadrupole moments are defined as [17]

$$Q_{\mu\nu}(\mathbf{r}_0) = \iint_S \frac{iz_0 k}{2} u_n(\mathbf{r}_s)(x_{s\mu} - x_{0\mu})(x_{s\nu} - x_{0\nu}) + p(\mathbf{r}_s)\hat{n}_\mu(x_{s\nu} - x_{0\nu})dS. \quad (6)$$

This equation allows for an expression for the three longitudinal ($\mu = \nu$) quadrupole moments for any expansion origin $\mathbf{r}_0$ in terms of the quadrpole, dipole, and monopole moments expanded about the origin as

$$Q_{\mu\mu}(\mathbf{r}_0) = Q^{(2)}_{\mu\mu}(\mathbf{0}) - x''_\mu D_\mu(\mathbf{0}) + \frac{1}{2}x''^2_\mu M. \quad (7)$$

In a similar fashion to the definition of the low-frequency acoustic center of an omnidirectional source, assume that expanding the pressure about the acoustic center causes the longitudinal quadrupole moments to vanish:

$$Q_{\mu\mu}(\mathbf{r}_c) = 0, \quad \mu = 1, 2, 3. \quad (8)$$

Then the dipole acoustic center follows by solving the quadratic equation of Eq. (7) as

$$x_{c\mu} = \frac{D_\mu(\mathbf{0}) \pm \sqrt{D_\mu(\mathbf{0})^2 - 2MQ_{\mu\mu}(\mathbf{0})}}{M}. \quad (9)$$

The choice of sign will be determined from physical considerations. The average of the two roots is

$$\frac{1}{2}(x_{c\mu}^{-} + x_{c\mu}^{+}) = \frac{D_\mu(\mathbf{0})}{M} = \mathbf{r}_c^{(o)}, \tag{10}$$

which is the equation of the acoustic center of an omnidirectional source [11].

One disadvantage of Eq. (9) is that for a purely dipolar source ($M = 0$), the equation for the acoustic center becomes singular. An alternative solution to the quadratic equation which overcomes this limitation is

$$x_{\mu c} = \frac{2Q_{\mu\mu}(\mathbf{0})}{D_\mu(\mathbf{0}) \pm \sqrt{D_\mu(\mathbf{0})^2 - 2MQ_{\mu\mu}(\mathbf{0})}}. \tag{11}$$

For a purely dipolar source, the acoustic center becomes

$$x_{\mu c} = \frac{Q_{\mu\mu}(\mathbf{0})}{D_\mu(\mathbf{0})}, \quad M = 0, \tag{12}$$

which is identical in form to the low-frequency acoustic center of an omnidirectional source.

2.2 Relation to Spherical Harmonic Expansion Coefficients

Calculating the acoustic center follows in a straightforward fashion from Eqs. (9) or (11). While in practice the multipole moments are generally unknown, they can be estimated from measured data using spherical harmonic expansion coefficients [11, 18, 19].

The relationship for the monopole and dipole moments are given in [11]. For the quadrupole moments, assume that the normal component of the particle velocity is known on a spherical surface of radius a. Then the normal particle velocity may be expanded in terms of spherical harmonics as

$$u_n(\theta,\phi) = \sum_{n=0}^{\infty}\sum_{m=-n}^{n} U_n^m Y_n^m(\theta,\phi), \tag{13}$$

where Y_n^m are the normalized spherical harmonics and U_n^m are the expansion coefficients. From Euler's equation, the surface pressure becomes [11]

$$p(a,\theta,\phi) = -iz_0 \sum_{n=0}^{\infty}\sum_{m=-n}^{n} U_n^m \frac{h_n^{(2)}(ka)}{h_n^{(2)'}(ka)} Y_n^m(\theta,\phi). \tag{14}$$

Substituting the expressions for the surface pressure and normal particle velocity into the definition of the quadrupole moment (Eq. (6)), applying the small-argument relations of the spherical Hankel functions [11]

$$\frac{h_n^{(2)}(ka)}{h_n^{(2)'}(ka)} \approx -\frac{ka}{(n+1)}, \quad ka << 1, \tag{15}$$

and simplifying yields

$$Q_{\mu\mu} = iz_0 ka^4 \sum_{n=0}^{\infty}\sum_{m=-n}^{n} U_n^m \left(\frac{n+3}{2n+2}\right) \times \int_0^{2\pi}\int_0^{\pi} \hat{x}_\mu^2 Y_n^m(\theta,\phi)\sin\theta d\theta d\phi, \quad ka << 1, \tag{16}$$

where $x_\mu = a\hat{x}_\mu$. The Wigner 3j symbols may be used to evaluate the integral as follows. First, let $(x_\mu)_n^m$ represent the spherical harmonic expansion coefficients of the unit vectors $\hat{x}$, $\hat{y}$, and $\hat{z}$, which are given in [11]. Then define

$$\begin{aligned} N_n^m(\hat{x}_\mu) &= \int_0^{2\pi}\int_0^{\pi} \hat{x}_\mu^2 Y_n^m(\theta,\phi)\sin\theta d\theta d\phi \\ &= \sum_{p=0}^{\infty}\sum_{p=-q}^{q}\sum_{s=0}^{\infty}\sum_{t=-s}^{s} (x_\mu)_p^q (x_\mu)_s^t \\ &\times \int_0^{2\pi}\int_0^{\pi} Y_p^q(\theta,\phi) Y_s^t(\theta,\phi) Y_n^m(\theta,\phi)\sin\theta d\theta d\phi. \end{aligned} \tag{17}$$

The integral over the sphere of the product of three spherical harmonics may be simplified as

$$N_n^m(\hat{x}_\mu) = \sum_{p=0}^{\infty}\sum_{p=-q}^{q}\sum_{s=0}^{\infty}\sum_{t=-s}^{s} (x_\mu)_p^q (x_\mu)_s^t \times \sqrt{\frac{(2n+1)(2p+1)(2s+1)}{4\pi}} \begin{pmatrix} n & p & s \\ 0 & 0 & 0 \end{pmatrix} \begin{pmatrix} n & p & s \\ m & q & t \end{pmatrix} \tag{18}$$

where the final two terms, which appear as 2×3 matrices, are the Wigner 3j symbols [20]. Evaluating these sums yields the coefficients for the expansions coefficients as

$$\begin{aligned} Q_{xx} &= iz_0 ka^4 \left(\sqrt{\pi}U_0^0 - \frac{1}{9}\sqrt{5\pi}U_2^0 + \frac{1}{2}\sqrt{\frac{5\pi}{6}}(U_2^{-2} + U_2^2)\right) \\ Q_{yy} &= iz_0 ka^4 \left(\sqrt{\pi}U_0^0 - \frac{1}{9}\sqrt{5\pi}U_2^0 - \frac{1}{2}\sqrt{\frac{5\pi}{6}}(U_2^{-2} + U_2^2)\right) \\ Q_{zz} &= iz_0 ka^4 \left(\sqrt{\pi}U_0^0 + \frac{2}{9}\sqrt{5\pi}U_2^0\right). \end{aligned} \tag{19}$$

For axisymmetric radiators, the equations simplify further to

$$\begin{aligned} M &= iz_0ka^2 4\pi V_0 \\ D_z(\mathbf{0}) &= iz_0ka^3 2\pi V_1 \\ Q_{zz}(\mathbf{0}) &= iz_0ka^4 2\pi(V_0 + \frac{2}{9}V_2), \end{aligned} \tag{20}$$

where V_n are the Legendre polynomial expansion coefficients of the surface normal velocity [11, 21]. The dipole acoustic center then becomes

$$r_c = a\frac{2(V_0 + \frac{2}{9}V_2)}{V_1 \pm \sqrt{V_1^2 - 4V_0(V_0 + \frac{2}{9}V_2)}}. \tag{21}$$

3. RESULTS

3.1 Axially Vibrating Cap on a Rigid Sphere

A first instructive model is an axially vibrating cap on a rigid sphere. Its normal surface velocity is defined as [21]

$$u_n(\theta, \phi) = \begin{cases} u_0 \cos\theta, & \theta \leq \theta_0 \\ 0, & \theta > \theta_0 \end{cases}, \tag{22}$$

where u_0 is the amplitude and θ_0 is the cap half-angle. This theoretical model has two important limiting cases. First, as $\theta_0 \to 0$, the source's sound field approaches the far-field omnidirectional radiation of a point source on a sphere. Second, as $\theta_0 \to \pi$, the source approximates a transversely oscillating sphere with far-field dipole radiation [17]. Consequently, this source can vary from purely monopole to purely dipole radiation depending on the chosen cap half-angle.

However, the shift from far-field omnidirectional to dipole radiation occurs over a relatively narrow range of cap values. Figure 1 demonstrates this transition by plotting the numerically evaluated Directivity Index (DI) [21] over θ_0 for $ka << 1$. The shift from a DI of 0 dB (omnidirectional radiation) to ≈ 4.77 dB (dipole radiation) occurs between 170° to 180° because the dipole moment becomes relatively stronger only when the net surface velocity (volume velocity) tends to zero due to the exact cancellation of the in and out-of-phase components of the sphere's vibration.

The source's directivity balloons reflect the trends seen in the DI plot. Figure 2 plots the far-field directivity for $ka = 0.001$ for select cap half-angles. Even for a cap half-angle of 177° (Fig. 2(a)), the radiation

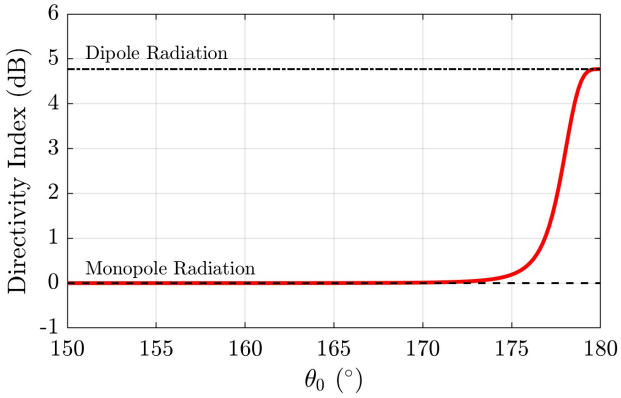

Figure 1. Directivity Index of an axially vibrating cap on a rigid sphere. For values of $0° \leq \theta_0 \leq 150°$, the DI is 0 dB (omnidirectional).

is quasi-omnidirectional. However, for a cap angle of 178° (Fig. 2(b)), a null begins to form in the xy-plane. As the monopole moment continues to vanish, the radiation appears more dipole-like until at 180° a perfect null forms in the xy-plane (Fig. 2(d)). Radiation patterns similar to those in Fig. 2(b)-(d) appear in measured results of ported loudspeakers, open back guitar amplifiers, and gongs [13–15], underscoring the utility of this theoretical model to predict dipole-like radiators.

The low-frequency acoustic center of this source follows from its spherical harmonic expansion coefficients. The expansion coefficients of the surface velocity are [11]

$$U_n^m = V_n \frac{4\pi[Y_n^m(\theta_0, \phi_0)]^*}{2n+1}, \tag{23}$$

where (θ_0, ϕ_0) is the direction of the cap and V_n are the expansion coefficients for the axisymmetric case $[(\theta_0, \phi_0) = (0, 0)]$. The axisymmetric coefficients are given for $0 \leq n \leq 2$ as [21]

$$V_n = \frac{u_0}{2}\begin{cases} \frac{1}{2}(1 - \cos^2\theta_0), & n = 0 \\ 1 - \cos^3\theta_0, & n = 1 \\ \frac{2}{3} - \frac{5}{21}P_2(\theta_0) - \frac{3}{7}P_4(\theta_0), & n = 2, \end{cases} \tag{24}$$

where P_n are the Legendre polynomials. Substituting these values into the axisymmetric relationships of Eq. (21) yields the dipole acoustic center.

It is informative to consider the two limiting cases of $\theta_0 \to 0°$ and $\theta_0 \to 180°$ before studying the full results.

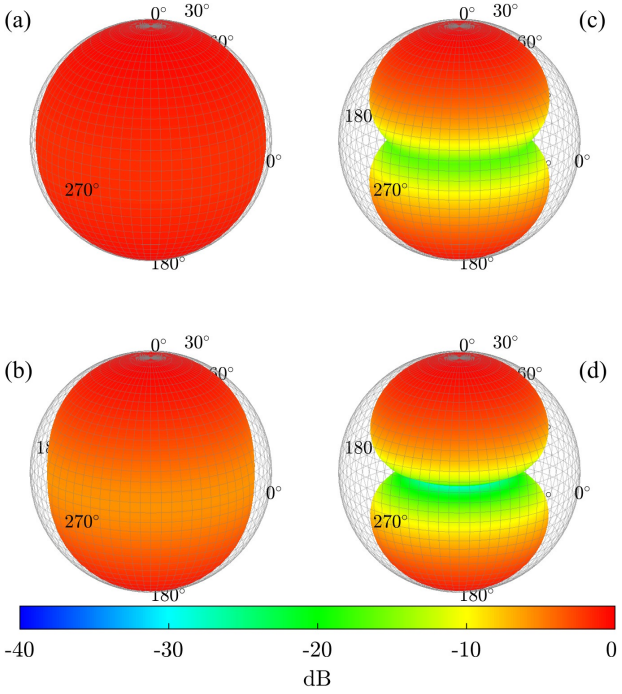

Figure 2. Far-field directivity pattern for an axially vibrating cap on a rigid sphere with cap half-angle (a) $\theta_0 = 177°$, (b) $\theta_0 = 178°$, (c) $\theta_0 = 179°$, and (d) $\theta_0 = 180°$. The cap is oriented to the positive z-axis.

The former condition, representative of a point source on a rigid sphere, has an acoustic center located at $1.5a$ [11]. The latter case, representative of a transversely oscillating sphere, must, by arguments of symmetry, have an acoustic center at the origin. Consequently, the physical solution must properly interpolate between these two limiting cases.

Curves representing the low-frequency acoustic center of an axially vibrating cap appear in Fig. 3. First, the solid red curve marked $r_c^{(o)}$ indicates the omnidirectional low-frequency acoustic center given in [11]. For cap half-angles of $0° \leq \theta_0 \leq 90°$, this definition is unambiguous because the surface velocity is all in-phase and positive. However, cap half-angles beyond $90°$ can accrue a significant dipole moment that weakens the underlying assumption of purely omnidirectional far-field radiation and makes the application of the definition more dubious. In fact, as $\theta_0 \to 180°$, the curve representing $r_c^{(o)}$ goes to infinity because the monopole moment goes to zero.

As the dipole moment strengthens with increasing cap

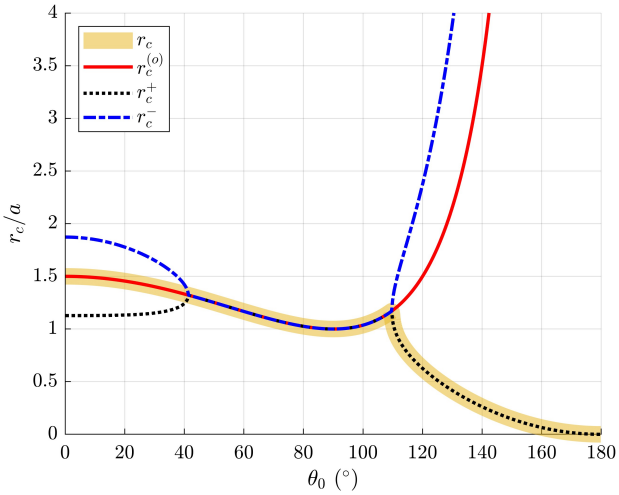

Figure 3. Acoustic center of an axially vibrating cap on a rigid sphere.

half-angle, incorporating both a monopole and dipole term to represent far-field radiation becomes necessary. The dashed blue curve and the dotted black curve represent the real parts of the negative and positive roots of the dipole acoustic center, respectively. The curves agree with the result expressed in Eq. (10) that the sum of the two roots must equal $r_c^{(o)}$. When considering the limiting condition that the acoustic center should approach the origin as $\theta_0 \to 180°$, only the positive root r_c^+ leads to a physically meaningful value for this source.

From approximately $45°$ to $110°$, the three solutions $r_c^{(o)}$, r_c^- and r_c^+ exactly agree. In this range, the terms inside the square root become negative so that the real part is simply $r_c^{(o)}$, as apparent from Eq. (9). For smaller cap half-angles, the dipole equation does provide real-valued solutions; however, because the far-field radiation at these angles is omnidirectional, incorporating dipole terms in the expansion is less meaningful.

Although a radially vibrating cap in a rigid sphere has well-defined radiation characteristics, determining its acoustic center is not straightforward. The bifurcations appearing in the graph indicate that physical intuition and knowledge of radiation trends must guide the choice of a proper center. For this source, the solid yellow highlight marks the acoustic center assuming that a single monopole is the appropriate model up until around $105°$, after which a monopole and dipole model becomes necessary.

The choice of source model does lead to different

characteristics in the radiated field after centering. Figure 4(a) plots the pressure field around the sphere for a cap angle of 126°, (compare Ref. [11], Fig. (6)). Although the far-field radiation is omnidirectional, the out-of-phase components of the surface velocity lead to cardiod-like patterns in the near-field. Figure 4(b) and (c) show the pressure field produced by a monopole at the omnidirectional acoustic center $r_c^{(o)}$ and a monopole and a dipole at the dipole acoustic center r_c^{+}, respectively.

Although both models show agreement with the source's far-field radiation, incorporating the dipole term leads to better near-field agreement. A surprising result is that the optimal location for a first-order and second-order expansion is different. Thus, simply defining the acoustic center as a location that minimizes a specific multipole moment may not be a robust approach, since an idealized source model should allow the inclusion or exclusion of higher-order terms without altering the expansion origin.

3.2 Two Point Sources on a Sphere

A second interesting theoretical case is two point sources on opposing sides of a rigid sphere with a varying amplitudes Q_s and γQ_s, where γ is a real number and represents the ratio of source strengths. As discussed in Sec. IV E of [11], this source becomes a dipole radiator when $\gamma = -1$, leading to a nonphysical omnidirectional low-frequency acoustic center position.

Assuming an axisymmetric configuration with the first point source with amplitude Q_s at $\mathbf{r} = a\hat{\mathbf{z}}$ and the second point source of amplitude γQ_s at $\mathbf{r} = -a\hat{\mathbf{z}}$, the spherical harmonic expansion coefficients of the source are given as [11]

$$U_n^0 = \frac{Q_s}{a^2}\sqrt{\frac{2n+1}{4\pi}}[1+\gamma(-1)^n]. \tag{25}$$

Figure 5 plots solutions to the acoustic center for this source, including the low-frequency monopole acoustic center $r_c^{(o)}$ and the two roots of the low-frequency dipole acoustic center $r_c^{\pm}$.

Similar to the case of an axially vibrating cap, considering the limiting cases is important to interpreting the results. In the regime $\gamma \geq 0$, the two point sources have positive amplitudes, are in-phase, and have no strong dipole moment. When the second point source is turned off ($\gamma = 0$) the acoustic center coincides with that of the isolated first point source at $r_c = 1.5a$. As $\gamma \to \infty$ so that the amplitude of the second point source is much

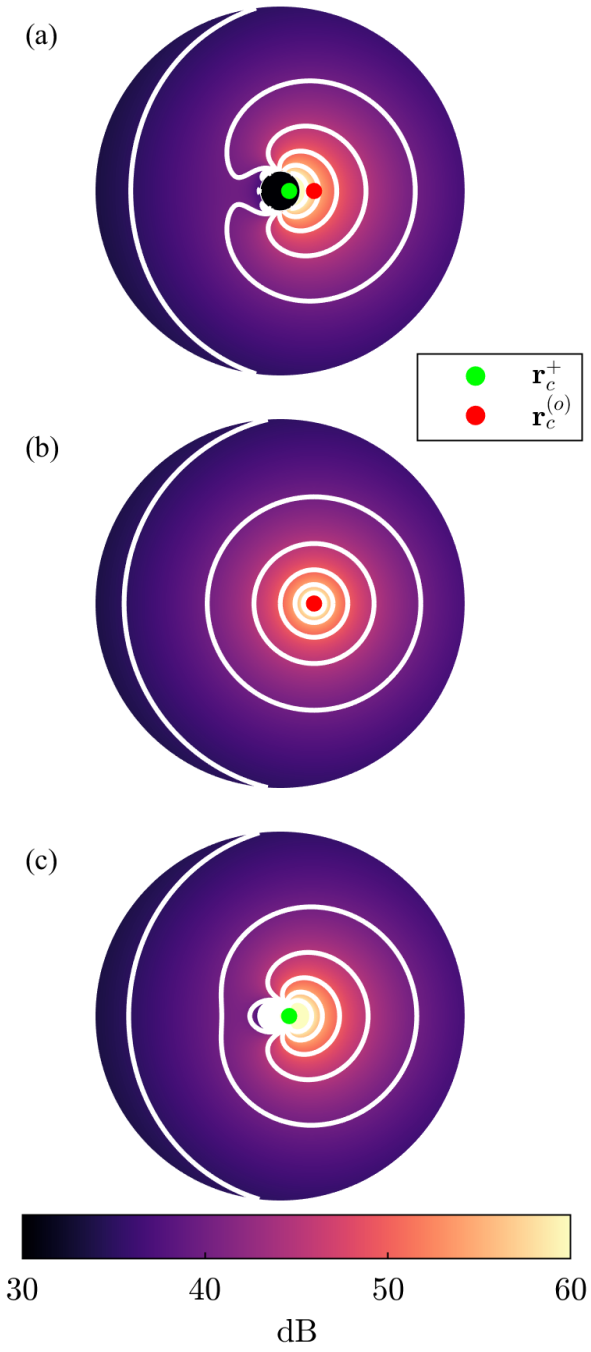

Figure 4. Sound pressure field produced by (a) and axially vibrating cap on a sphere with $\theta_0 = 126°$, (b) a single monopole located at $r_c^{(o)}$, and (c) a monopole and dipole located at r_c^{+}.

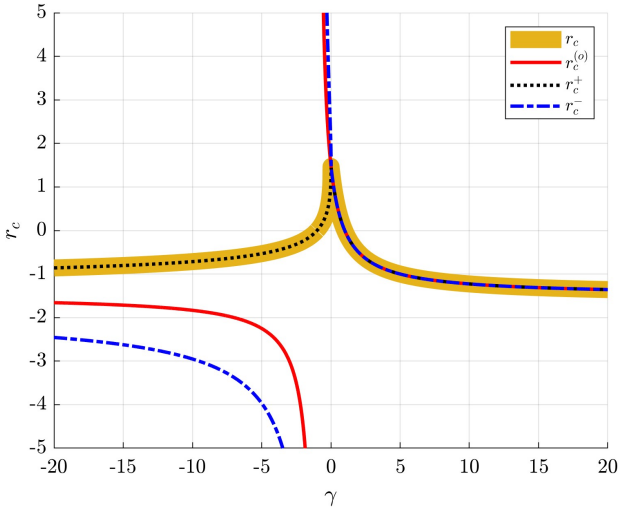

Figure 5. Acoustic center for two point sources at the opposing poles of a sphere.

greater than that of the first, the acoustic center asymptotically approaches that of the isolated second point source at $r_c = -1.5a$. Lastly, when $\gamma = 1$ so that the point source amplitudes are equal, by arguments of symmetry the acoustic center should fall at the origin. Both $r_c^{(o)}$ and the real parts of $r_c^{\pm}$ concur with these conditions.

However, when $\gamma < 0$, two other important limiting cases must occur. When $\gamma = -1$, the monopole moment is zero and the the far-field radiation is purely dipolar. By arguments of symmetry, the acoustic center must fall at the origin. Lastly, as $\gamma \to -\infty$, the acoustic center must again asymptotically converge to that of the isolated second point source at $r_c = -1.5a$. Because only the dipole center r_c^+ satisfies these conditions, r_c^+ is the physical solution for $\gamma < 0$.

4. DISCUSSION

The absence of a consistent definition for the acoustic center hinders the development of reliable identification algorithms. A coherent definition only emerges at large wavelengths and for sources exhibiting omnidirectional radiation. As noted by Jacobsen et al. [7], generalizing the concept of an acoustic center to sources with directional radiation is a significant challenge. Although this work extended the low-frequency acoustic center to sources with dipole components in their far-field radiation, the results illustrate several remaining obstacles and ambiguities.

For example, while the omnidirectional low-frequency acoustic center yields a single linear equation with a unique solution, incorporating second-order dipole terms leads to quadratic equations with two distinct roots for each Cartesian direction. Including higher-order terms will result in higher-order algebraic equations, requiring the isolation of a single physically meaningful solution. While theoretical models allow for the observation of key limiting behaviors to identify the correct solution, such information is often absent for real, measured sources, posing significant practical challenges for higher-order sources.

Another ambiguity arises from the influence of the source model on the acoustic center. The example of an axially vibrating cap on a sphere, as illustrated in Fig. 4, suggests that even for the same source, the acoustic center's location varies depending on whether dipole terms are included. Ideally, the expansion point should be independent of the source model, allowing for the flexible incorporation of higher-order terms. Furthermore, the criteria for choosing between a monopole model and a monopole-dipole model remain unclear. While one might assume that far-field radiation characteristics will always determine this choice, the results in Fig. 4, corresponding to omnidirectional radiation (DI $\approx$ 0 dB), showed better near-field agreement with the dipole model. This finding implies that the optimal definition and model for the acoustic center may be application-dependent, requiring consideration of specific needs such as near-field accuracy versus far-field source behavior.

5. CONCLUSIONS

This work explored the extension of the low-frequency acoustic center to dipole radiators through a multipole expansion of the Kirchhoff-Helmholtz Integral Equation. The resultant theory overcame previous limitations for source configurations with dipole radiation characteristics, including producing a physical location of the acoustic center and improved near-field agreement. Future work includes applying the method to more theoretical models and measured results as well as validating the technique with previously proposed algorithms.

6. ACKNOWLEDGMENTS

The William James and Charlene Fuhriman Strong Family Endowed Fellowship Fund for Musical Acoustics supported this work.

7. REFERENCES

[1] M. Vorländer and H. Bietz, "Novel broad-band reciprocity technique for simultaneous free-field and diffuse-field microphone calibration," *Acta Acust. Acust.*, vol. 80, pp. 365–367, July 1994.

[2] R. P. Wagner and V. Nedzelnitsky, "Determination of acoustic center correction values for type ls2ap microphones at normal incidence," *J. Acoust. Soc. Am.*, vol. 104, no. 1, pp. 192–203, 1998.

[3] S. Barrera-Figueroa, K. Rasmussen, and F. Jacobsen, "The acoustic center of laboratory standard microphones," *J. Acoust. Soc. Am.*, vol. 120, no. 5, pp. 2668–2675, 2006.

[4] K. A. Cunefare, V. B. Biesel, J. Tran, R. Rye, A. Graf, M. Holdhusen, and A.-M. Albanese, "Anechoic chamber qualification: Traverse method, inverse square law analysis method, and nature of test signal," *J. Acoust. Soc. Am.*, vol. 113, no. 2, pp. 881–892, 2003.

[5] D. Deboy, "Acoustic centering and rotational tracking in surrounding spherical microphone arrays," *Master's thesis, Institute of Electronic Music and Acoustics, University of Music and Performing Arts, Graz, Austria*, 2010.

[6] I. Ben Hagai, M. Pollow, M. Vorländer, and B. Rafaely, "Acoustic centering of sources measured by surrounding spherical microphone arrays," *J. Acoust. Soc. Am.*, vol. 130, no. 4, pp. 2003–2015, 2011.

[7] F. Jacobsen, S. B. Figueroa, and K. Rassmussen, "A note on the concept of acoustic center," *J. Acoust. Soc. Am.*, vol. 115, no. 4, pp. 1468 – 1473, 2004.

[8] *IEC 61094-3: Electroacoustics-Measurement microphones-Part 3: Primary method for free-field calibration of laboratory standard microphones by the reciprocity technique*. International Electrotechnical Commission (IEC), June 2016.

[9] *ANSI S1.1-1994 (r2004): American National Standard Acoustical Terminology*. American National Standards Institute, Inc., March 2004.

[10] J. Vanderkooy and D. Henwood, "Polar plots for low frequencies: The acoustic centre," in *Audio Engineering Convention 120*, (Paris, France), May 2006.

[11] S. D. Bellows and T. W. Leishman, "On the low-frequency acoustic center," *J. Acoust. Soc. Am.*, vol. 153, pp. 3404–3418, June 2023.

[12] S. D. Bellows, "Acoustic directivity: Advances in acoustic center localization, measurement optimization, directional modeling, and sound power spectral estimation.," *Doctoral Dissertation, Brigham Young University, Provo, Utah, USA*, 2023.

[13] S. D. Bellows and T. W. Leishman, "Obtaining far-field spherical directivities of guitar amplifiers from arbitrarily shaped arrays using the Helmholtz equation least-squares method," *Proc. Meet. Acoust.*, vol. 42, no. 1, p. 055005, 2020.

[14] S. D. Bellows and T. W. Leishman, "Low-frequency radiation from a vibrating cap on a rigid spherical shell with a circular aperture," *J. Acoust. Soc. Am.*, vol. 154, pp. 3883–3898, Dec. 2023.

[15] S. D. Bellows, D. T. Harwood, K. L. Gee, and M. R. Shepherd, "Directional characteristics of two gamelan gongs," *J. Acoust. Soc. Am.*, vol. 154, pp. 1921–1931, Sept. 2023.

[16] G. Weinreich, "Sound hole sum rule and the dipole moment of the violin," *J. Acoust. Soc. Am.*, vol. 77, no. 2, pp. 710–718, 1985.

[17] A. D. Pierce, *Acoustics*. Springer International Publishing, 2019.

[18] E. G. Williams, *Fourier Acoustics: Sound Radiation and Nearfield Acoustical Holography*. London: Academic Press, 1999.

[19] T. Martin and A. Roure, "Optimization of an active noise control system using spherical harmonics expansion of the primary field," *J. Sound Vib.*, vol. 201, no. 5, pp. 577–593, 1997.

[20] R. Kennedy and P. Sadeghi, *Hilbert Space Methods in Signal Processing*. Cambridge University Press, 2013.

[21] L. Beranek and T. Mellow, *Acoustics: Sound fields, transducers and vibration*. Academic Press, 2 ed., 2019.